

## Characterization of the thyroid $\text{Na}^+/\text{I}^-$ symporter with an anti-COOH terminus antibody

ORLIE LEVY, GE DAI, CLAUDIA RIEDEL, CHRISTOPHER S. GINTER, ELLIOT M. PAUL, ADAM N. LEBOWITZ, AND NANCY CARRASCO\*

Department of Molecular Pharmacology, Albert Einstein College of Medicine, Bronx, NY 10461

Communicated by H. Ronald Kaback, University of California, Los Angeles, CA, March 14, 1997 (received for review January 24, 1997)

**ABSTRACT** The  $\text{Na}^+/\text{I}^-$  symporter (NIS) is the plasma membrane protein that catalyzes active  $\text{I}^-$  transport in the thyroid, the first step in thyroid hormone biogenesis. The cDNA encoding NIS was recently cloned in our laboratory and a secondary structure model proposed, suggesting that NIS is an intrinsic membrane protein (618 amino acids;  $\approx 65.2$  kDa predicted molecular mass) with 12 putative transmembrane domains. Here we report the generation of a site-directed polyclonal anti-COOH terminus NIS antibody (Ab) that immunoreacts with a  $\approx 87$  kDa-polypeptide present in membrane fractions from a rat thyroid cell line (FRTL-5). The model-predicted cytosolic-side location of the COOH terminus was confirmed by indirect immunofluorescence experiments using anti-COOH terminus NIS Ab in permeabilized FRTL-5 cells. Immunoreactivity was competitively blocked by the presence of excess synthetic peptide. Treatment of membrane fractions from FRTL-5 cells, *Xenopus laevis* oocytes, and COS cells expressing NIS with peptidyl *N*-glycanase F converted the  $\approx 87$  kDa-polypeptide into a  $\approx 50$  kDa-species, the same relative molecular weight exhibited by NIS expressed in *E. coli*. Anti-NIS Ab immunoprecipitated both the NIS precursor molecule ( $\approx 56$  kDa) and the mature  $\approx 87$  kDa form. Furthermore, a direct correlation between circulating levels of thyroid-stimulating hormone and NIS expression *in vivo* was demonstrated.

NIS ( $\text{Na}^+/\text{I}^-$  symporter) is a key plasma membrane protein that catalyzes the active accumulation of iodide ( $\text{I}^-$ ) in the thyroid gland, a major step in the biosynthesis of thyroid hormones thyroxine ( $\text{T}_4$ ) and tri-iodothyronine ( $\text{T}_3$ ). These hormones are involved in regulating intermediary metabolism in virtually all tissues, and in the maturation of the nervous system, skeletal muscle, and lungs in the developing fetus and the newborn (1, 2). NIS plays a crucial role in the evaluation, diagnosis, and treatment of various thyroid pathological conditions (3, 4), because it is the molecular basis for radioiodide thyroid-imaging techniques and for specific targeting of radioisotopes to the gland. NIS couples the inward translocation of  $\text{Na}^+$  down its electrochemical gradient to the simultaneous inward “uphill” translocation of  $\text{I}^-$  against its electrochemical gradient (reviewed in ref. 5). The  $\text{Na}^+$  gradient that provides the driving force for  $\text{I}^-$  uptake is maintained by the  $\text{Na}^+/\text{K}^+$  ATPase.

The cDNA encoding NIS was recently cloned by functional screening of a cDNA library from a rat thyroid-derived cell line (FRTL-5 cells) in *Xenopus laevis* oocytes (6). The proposed secondary structure model suggests that NIS is an intrinsic membrane protein ( $\approx 65.2$  kDa predicted molecular weight) with 12 putative transmembrane domains (6, 7). The model

predicts that both the amino and C termini are located on the intracellular side of the membrane (5, 7). However, such model predictions regarding orientation and topology of NIS with respect to the plasma membrane have yet to be confirmed experimentally, and structure/function studies remain to be performed to elucidate the molecular mechanism of NIS activity. Until recently, a major limitation on efforts to further characterize NIS was the unavailability of anti-NIS antibodies (Abs). In this study we report the generation of a site-directed polyclonal anti-C-terminal NIS Ab that immunoreacted with various NIS polypeptide species. Using this Ab we have: (i) confirmed experimentally that the C terminus of NIS is, as predicted, on the cytoplasmic side of the membrane, (ii) examined N-linked glycosylation of NIS, (iii) determined the molecular mass and monitored the maturation of the NIS precursor molecule, and (iv) demonstrated a direct correlation between circulating levels of thyroid-stimulating hormone (TSH) and NIS expression in the thyroid *in vivo*. It is clear that the continued elucidation of structural domain topology of NIS is required for the future design of studies to identify the sodium and iodide binding/translocation sites on the NIS molecule.

### MATERIALS AND METHODS

**Synthesis of the NIS C-Terminal Peptide.** A peptide corresponding to C-terminal sequence of NIS, amino acids 603–618: AETHPLYLGHVETNL was synthesized by solid phase synthesis (8). The peptide was purified by reversed-phase HPLC on a C-18 column. The purity of the peptide was assessed by amino acid analysis.

**Conjugation of the C-Terminal Peptide to Keyhole Limpet Hemocyanin (KLH).** The C-terminal peptide was coupled to the carrier molecule KLH by incubating overnight, at  $4^\circ\text{C}$ ,  $3.4$   $\mu\text{mol}$  of peptide with  $0.5$  nmol of KLH in the presence of  $20$   $\mu\text{mol}$  of glutaraldehyde followed by overnight dialysis against PBS ( $137$  mM NaCl/ $2.4$  mM KCl/ $10.4$  mM  $\text{Na}_2\text{HPO}_4$ / $1.8$  mM  $\text{KH}_2\text{PO}_4$ , pH 7.2).

**Antibody Production.** Ab was obtained by immunizing female New Zealand White rabbits with  $0.5$  mg of C-terminal peptide/KLH conjugate emulsified in complete Freund's adjuvant. The mixture was injected intradermally at  $\approx 4$  sites and the animals were administered booster injections 5 weeks later by intradermal injections of the same amount of conjugate in incomplete Freund's adjuvant. Blood samples were obtained  $\approx 10$ – $14$  days thereafter.

**Purification of Anti-NIS Antibody.** The C-terminal peptide was coupled to an Affi-Gel 15 column (Bio-Rad) and was used to purify the antibody as described in ref. 8.

The publication costs of this article were defrayed in part by page charge payment. This article must therefore be hereby marked “advertisement” in accordance with 18 U.S.C. §1734 solely to indicate this fact.

Copyright © 1997 by THE NATIONAL ACADEMY OF SCIENCES OF THE USA  
0027-8424/97/945568-6\$2.00/0  
PNAS is available online at <http://www.pnas.org>.

Abbreviations: NIS,  $\text{Na}^+/\text{I}^-$  symporter; Ab, antibody; TSH, thyroid-stimulating hormone; LDS, lithium-dodecyl sulfate; KLH, keyhole limpet hemocyanin; FRTL-5, Fisher rat thyroid; IPTG, isopropyl  $\beta$ -D-thiogalactopyranoside; PTU, 6-propyl-2-thiouracil.

\*To whom reprint requests should be addressed. e-mail: carrasco@acom.yu.edu.

**Growth of Cells.** FRTL-5 and FRT cells derived from Fisher rat thyroids (9) were cultured as originally reported (10). *X. laevis* oocytes and COS cells were cultured as described (6).

**Transport Assays.** FRT and FRTL-5 membrane vesicles were assayed exactly as described in ref. 11.

**Immunoblot Analysis.** SDS/9% PAGE and electroblotting to nitrocellulose were performed as previously described (11). All samples were diluted 1:2 with loading buffer and heated at 37°C for 30 min prior to electrophoresis. Immunoblot analyses were also carried out as described (11), with a 1:2,000 dilution of anti-NIS containing sera, and a 1:1,500 dilution of a horseradish peroxidase-linked donkey anti-rabbit IgG (Amersham). Both incubations were performed for 1 hr. Proteins were visualized by an enhanced chemiluminescence Western blot detection system (Amersham).

**Membrane Preparations from FRTL-5 Cells and NIS-Expressing *X. laevis* Oocytes and COS Cells.** Membranes from FRTL-5 cells were prepared with protease inhibitors as described (11). Microinjection of NIS cRNA and transfection of COS cells with NIS cDNA were performed as reported (6). Four days after microinjection *X. laevis* oocyte membranes were isolated as follows:  $\approx 40$  oocytes were homogenized in 200  $\mu$ l of a buffer containing 250 mM sucrose, 10 mM HEPES-KOH (pH 7.5), 1 mM EDTA, 1 mM phenylmethylsulfonyl fluoride (PMSF), 10  $\mu$ g/ml leupeptin, and 10  $\mu$ g/ml aprotinin (Sigma). The yolk was pelleted at 1,000  $\times g$  for 5 min. Twenty microliters of 1 M Na<sub>2</sub>CO<sub>3</sub> were added to the resulting supernatant and the sample was incubated at 4°C for 45 min (shaking). Membranes were then pelleted in an airfuge at 100,000  $\times g$  for 15 min. COS cells were transfected with 3  $\mu$ g per 10-cm plate NIS cDNA in pSV.SPORT (GIBCO/BRL) and harvested 2 days after transfection. Membranes from COS cells were isolated exactly as described for FRTL-5 cells with protease inhibitors (11).

**Expression of NIS in *E. coli*.** An oligonucleotide probe was constructed (5'-TCACCTGTCCATATGGAGGGTGC-3') to delete the 5' untranslated region and introduce an *Nde*I site at the initiation codon (Met pos 1). NIS cDNA was then subcloned into pET 28c(+) vector (Novagen) and transformed into BL21(DE3) strain (GIBCO/BRL). An overnight culture of cells was diluted 1:40 and grown until OD<sub>600nm</sub> reached 0.7. Subsequently, cells were induced with 0.5 mM isopropyl  $\beta$ -D-thiogalactopyranoside (IPTG) for 2 hr. Cells were pelleted and membranes were prepared as described in ref. 8.

**Peptidyl N-glycanase F Treatment.** Membranes were treated with N-glycanase following a modification of the manufacturer's protocol (Genzyme). Membranes ( $\approx 50$ –100  $\mu$ g) were resuspended in 10  $\mu$ l 0.5 M Tris-HCl pH 8.0 and 18.8  $\mu$ l of water was added either with 1.2  $\mu$ l N-glycanase (333 milliunits, Genzyme) or 1.2  $\mu$ l of 50% glycerol. Membranes were then incubated overnight at 37°C (18 hr). When treatment was done in the presence of lithium-dodecyl sulfate (LDS), 1.5  $\mu$ l of 2% LDS was added to the membranes. After the overnight incubation, the reaction was diluted 1:2 with loading buffer (15  $\mu$ l) and samples incubated at 37°C for 30 min prior to electrophoresis.

**Immunofluorescence.** FRTL-5 or FRT cells were seeded onto poly-(lysine) coated coverslips. When cells reached 40–50% confluence they were fixed with 4% paraformaldehyde for 10 min then washed three times with 1 $\times$  PBS. Cells were permeabilized with methanol for 5 min and washed three times with 1 $\times$  PBS. Cells were then blocked with 4% BSA/PBS for 1 hr and subsequently incubated with anti-NIS Ab at 1:500 dilution in 4% BSA/PBS for 1 hr. Cells were washed 3 times for 5 min with 0.2% Tween-20 in 1 $\times$  PBS and once with 1 $\times$  PBS only. Coverslips were then transferred onto 150  $\mu$ l 1 $\times$  PBS containing anti-rabbit fluorescein conjugated secondary Ab (1:100 dilution; Pierce) for 1 hr in the dark and then washed as above. Coverslips were air-dried for 3 min and were then mounted onto slides containing 15  $\mu$ l 1 $\times$  PBS in 50% glycerol with phenylenediamine. Coverslips were sealed with quick-dry

nailpolish and allowed to dry in the dark for 2 hr at room temperature and then stored at 4°C. Cells were visualized with a Nikon Diaphot microscope equipped for epifluorescence studies through a Nikon  $\times 100$  oil-immersion lens. Images were photographed using Kodak-Ektachrome 400 film.

**<sup>35</sup>S Labeling of FRTL-5 Cells and Immunoprecipitation with Anti-NIS Antibody.** FRTL-5 cells were washed and incubated with methionine-free RPMI 1640 medium supplemented with six hormones (10) for 30 min. Cells were labeled with 480  $\mu$ Ci/ml [<sup>35</sup>S]methionine/cysteine (Promix, Amersham) for 5 min followed by incubation with regular media supplemented with 10 $\times$  unlabeled methionine/cysteine for the indicated times. Cells were lysed in 1% SDS/1 $\times$  PBS for 5 min on ice, followed by a 16-fold dilution with 50 mM Tris-HCl, pH 7.5/1% Triton X-100/1% deoxycholate/200 mM NaCl/1% BSA. Pre-immune sera was added at a 1:40 dilution and incubated at 4°C for 30 min, followed by the addition of 1/7th volume of a 50% slurry of protein G fast flow Sepharose beads (Bio-Rad) incubated at 4°C for 30 min. Lysate was centrifuged at 14,000  $\times g$  for 5 min. Supernatants were centrifuged at 100,000  $\times g$  for 30 min. Anti-NIS sera was added at a 1:40 dilution, incubated at 4°C for 90 min, followed by the addition of 1/7th volume of a 50% slurry of protein G fast flow Sepharose beads incubated at 4°C for 60 min. Beads were centrifuged at 14,000  $\times g$  for 5 min. Beads were washed alternately three times with low- and high-ionic strength buffers (10 mM Tris-HCl, pH 7.5/150 mM NaCl/1% Triton X-100/1% deoxycholate/1 mM EDTA; the high ionic strength buffer is the same plus 0.5 M LiCl). The final wash was done with 10 mM Tris-HCl (pH 7.5). Beads were heated at 37°C in loading buffer prior to SDS electrophoresis. After gels were fixed, they were washed extensively with water and soaked in Fluoro-Hance (Research Products International) for 30 min. Gels were vacuum dried and exposed for autoradiography at  $-80^\circ\text{C}$ .

**In Vivo Regulation of NIS by TSH.** Experimental hypothyroidism was induced by addition of 0.05% (wt/vol) of the antithyroid agent 6-propyl-2-thiouracil (PTU) to the rats drinking water for 2 weeks. A separate group of rats was subjected to an iodine deficient diet (Harlan-Teklad) for 2–4 weeks. Hypophysectomized rats were obtained from Charles River Breeding Laboratories. Bovine TSH (1 unit) was subsequently injected into hypophysectomized rats. Thyroidectomies of experimental and control rats were performed, and thyroid membrane fractions were prepared for immunoblot analysis (11) with anti-NIS Ab.

## RESULTS AND DISCUSSION

**Generation of an Anti-COOH Terminus NIS Ab.** A peptide corresponding in sequence to the last segment of the COOH terminus of NIS was synthesized (Fig. 1A). The synthetic peptide was coupled to the carrier molecule KLH and the conjugate was injected into rabbits. Blood samples were obtained 6 weeks after injection of the conjugate and sera were screened by immunoblot analysis. Both intact and Na<sub>2</sub>CO<sub>3</sub>-extracted membrane fractions from FRTL-5 cells were subjected to NaDodSO<sub>4</sub>/polyacrylamide electrophoresis; polypeptides were electrotransferred to nitrocellulose and probed with the antisera. Na<sub>2</sub>CO<sub>3</sub>-extracted fractions were used because they are enriched in integral membrane proteins. Reactivity of the anti-COOH NIS Ab was demonstrated with a polypeptide of  $\approx 87$  kDa relative molecular weight in both membrane preparations (Fig. 1B, lanes 1 and 3). Tellingly, immunoreactivity was more pronounced in Na<sub>2</sub>CO<sub>3</sub>-extracted membranes [Fig. 1B (compare lane 3 with lane 1)], suggesting that the immunoreactive polypeptide is an integral membrane protein. Immunoreactivity was competitively prevented by the synthetic peptide (Fig. 1B, lanes 2 and 4), demonstrating that the Ab was recognizing its predetermined epitope on the  $\approx 87$

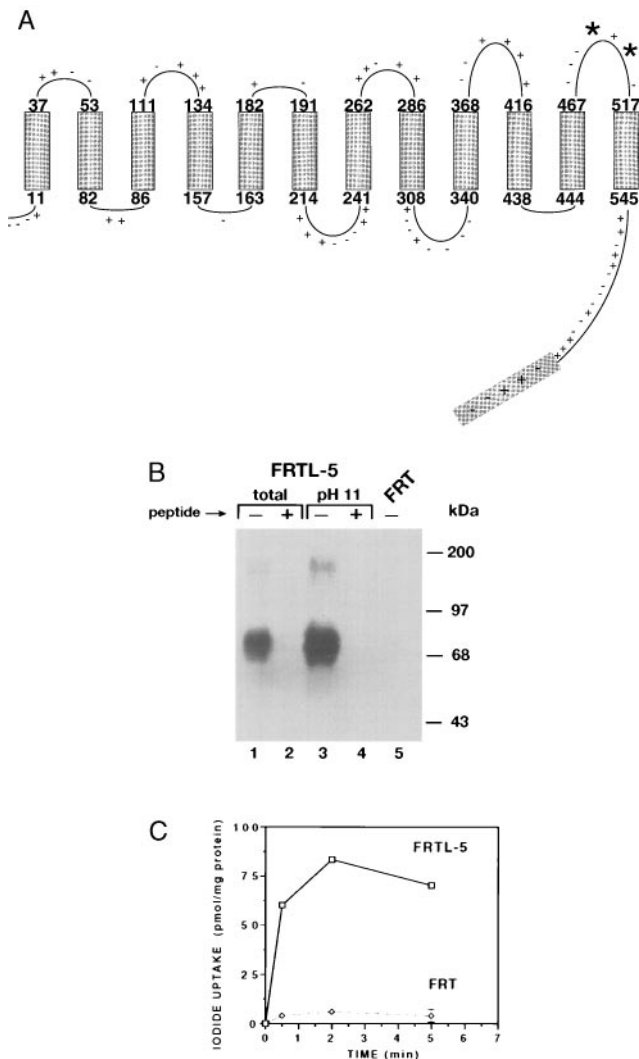


FIG. 1. (A) NIS secondary structure model. Putative rat NIS topology is shown as predicted on the basis of amino acid sequence (6). The 12 putative transmembrane domains are indicated by rectangles. Potential N-linked glycosylation sites are indicated by boldface asterisks. The C terminus region against which the anti-NIS Ab was generated is shaded. (B) Immunoblot analysis of FRTL-5 membranes with anti-NIS Ab. FRTL-5 and FRT membranes were isolated, electrophoresed, and electrotransferred onto nitrocellulose as described. Immunoblot analysis with anti-NIS Ab was conducted as described. Lanes 1 and 2, total FRTL-5 membranes ( $\approx 20 \mu\text{g}$ ); lanes 3 and 4, FRTL-5  $\text{Na}_2\text{CO}_3$  (pH 11) extracted membranes ( $\approx 20 \mu\text{g}$ ); lane 5, FRT total membranes ( $\approx 20 \mu\text{g}$ ). Lanes 2 and 4 had  $100 \mu\text{g}$  of peptide present during incubation with anti-NIS Ab. (C) Membrane vesicles were prepared from FRT and FRTL-5 cells and assayed as described (11). Shown is a time course of iodide uptake in membrane vesicles from FRTL-5 ( $\square$ ) and FRT cells ( $\diamond$ ) done in the presence of  $\text{Na}^+$ . Points indicate average of triplicate determinations.

kDa-polypeptide, and thus indicating that this polypeptide is NIS. It seems likely that the difference between the molecular weight of the immunoreactive polypeptide ( $\approx 87$  kDa) and the predicted molecular weight of NIS ( $\approx 65.2$  kDa) is due to such posttranslational modifications as glycosylation. Therefore, the observed  $\approx 87$  kDa molecular weight is consistent with the notion that the immunoreactive polypeptide is NIS. In addition, immunoreactivity was occasionally observed with a  $\approx 180$  kDa-polypeptide, conceivably a NIS dimer species. Significantly, no immunoreactivity was detected with polypeptides from FRT cells (Fig. 1B, lane 5), a line of rat thyroid-derived cells that exhibits no NIS activity (Fig. 1C). This observation shows that the lack of  $\text{I}^-$  transport activity in these cells is due

to the absence of NIS, a notion further confirmed by the immunofluorescence experiments (Fig. 2J).

**Corroboration of the Predicted Cytosolic-Side Location of the NIS COOH-Terminus Domain by Immunofluorescence.** Our secondary structure model (6, 7) predicts that the COOH-terminus domain of NIS is located on the cytosolic side of the membrane (Fig. 1A). This prediction was partly based on the fact that the COOH terminus contains a large hydrophilic region of  $\approx 70$  amino acids within which the only potential cAMP-dependent protein kinase A phosphorylation domain of the molecule is found (positions 549–552). To test this prediction, indirect immunofluorescence experiments were conducted in  $\text{I}^-$  transporting FRTL-5 cells and in non- $\text{I}^-$  transporting FRT cells. Intact or permeabilized cells were incubated with pre-immune or immune serum followed by fluorescein-conjugated second Ab. As shown in Fig. 2, when intact FRTL-5 cells were incubated with immune serum, a diffuse background was observed (Fig. 2B). In contrast, when FRTL-5 cells incubated with immune serum were permeabilized with methanol, the cells displayed membrane-associated fluorescence (Fig. 2D), which was abolished by addition of the COOH-terminus synthetic peptide (Fig. 2F). Staining was absent in permeabilized FRT cells incubated with immune serum (Fig. 2J), and in permeabilized FRTL-5 cells incubated

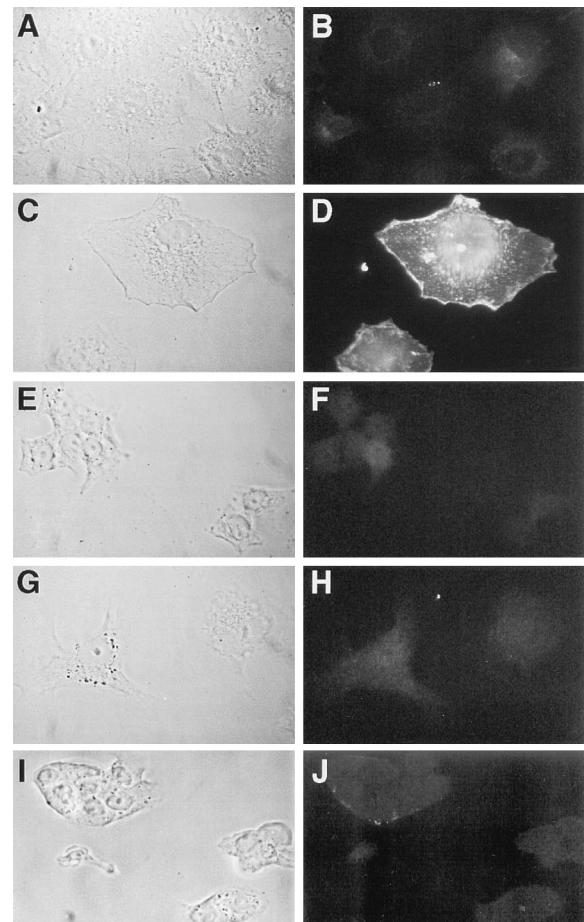


FIG. 2. Indirect immunofluorescence of FRTL-5 and FRT cells using anti-NIS Ab. FRTL-5 and FRT cells were cultured as described previously (10). Cells were trypsinized, harvested, and seeded onto poly-(lysine)-coated coverslips ( $\approx 50\%$  confluence). Next day cells were fixed in 4% paraformaldehyde and incubated either in the presence of anti-NIS Ab (1:500 B, D, F, J) or pre-immune (H) or in the presence (D, F, H, J) or absence (B) of methanol to expose intracellular antigen. Cells in F were incubated with  $20 \mu\text{g}$  of peptide. (Left) Phase contrast images (A, C, E, G, and I) of Right side (B, D, F, H, and J). Cells were visualized as described in Materials and Methods.

with pre-immune serum (Fig. 2H). The *Left* side shows the corresponding phase-contrast fields. Because methanol permeabilization makes the cytosolic side of the plasma membrane accessible to the Ab, these results clearly confirm the predicted cytosolic face location of the COOH terminus of NIS, and also represent the first reported visualization of NIS *in situ*.

**Analysis of N-Linked Glycosylation of NIS.** Immunoblot analysis was also carried out with membranes from *X. laevis* oocytes microinjected either with water or NIS cRNA (Fig. 3A, lanes 2 and 3, respectively). Immunoreactivity was observed predominantly with  $\approx 55$ -kDa and  $\approx 110$ -kDa polypeptide spe-

cies and occasionally with two other polypeptides of  $\approx 87$  kDa and  $\approx 180$  kDa. These molecular weights are compatible, respectively, with the putative nonglycosylated or partially processed NIS, its dimer, and posttranslationally processed NIS and its dimer. As expected, no immunoreactive polypeptides were detected in membranes from water-injected oocytes. Immunoreactivity was competitively blocked by incubation of serum in the presence of the COOH synthetic peptide (data not shown). These results strongly reinforce the notion that the polypeptides identified with the Ab are different species of NIS. Moreover, it is not surprising to find both partially and fully processed NIS in oocytes, given that oocytes are a heterologous expression system in which posttranslational modifications occur, although with some differences with respect to the native system.

When the NIS cDNA is transfected into COS cells, it elicits significant  $\text{Na}^+$  dependent,  $\text{ClO}_4^-$  sensitive  $\text{I}^-$  uptake activity (6). An immunoblot analysis of COS cells transfected with NIS cDNA revealed a prominent  $\approx 87$  kDa polypeptide, as well as three other polypeptide species, molecular weights  $\approx 55$ ,  $\approx 110$ , and  $\approx 180$  kDa (Fig. 3A, lane 5). No immunoreactive species was observed in untransfected COS cells (Fig. 3A, lane 4). Notably, the presumed nonprocessed NIS species (i.e., the  $\approx 55$ -kDa polypeptide species and its dimer) were not detected in immunoblots of membrane fractions from FRTL-5 cells in which NIS is an endogenous protein (Fig. 3A, lane 1). The  $\approx 55$  kDa molecular weight of the polypeptide detected in oocytes and COS cells is closer to the predicted 65.2 kDa molecular weight for NIS. Thus, the observed differences in molecular weights of the immunoreactive polypeptides may be due to differences in posttranslational processing of NIS between the various cell types examined. Remarkably, an  $\text{I}^-$  concentration gradient of  $\approx 30$ -fold is generated by NIS in all three systems, FRTL-5 cells (10, 11), COS cells (6), and oocytes (6), indicating that such differences in posttranslational processing are not major factors affecting NIS activity.

Three potential Asn-glycosylation sites are present in NIS at positions 225, 485, and 497. The last two are located in the 12th hydrophilic sequence, a domain predicted to be on the extracellular face of the membrane (Fig. 1A, asterisks). To test the hypothesis that the  $\approx 87$  kDa is glycosylated NIS, membrane fractions from FRTL-5 cells were subjected to treatment with peptidyl *N*-glycanase F, an enzyme that cleaves all N-linked oligosaccharides. Standard protocols for *N*-glycanase treatment include use of the detergents SDS and Nonidet P-40 as a means to unfold the proteins to be treated. However, use of these detergents caused pronounced aggregation of NIS. Therefore, *N*-glycanase treatment was performed either in the absence of detergents or in the presence of a low concentration (0.1%) of LDS. When detergents were absent, oligomerization of NIS was markedly decreased and a broad polypeptide band of  $\approx 69$  kDa was observed in the immunoblot (Fig. 3B, lane 2). In the presence of LDS, *N*-glycanase treatment yielded an  $\approx 50$ -kDa polypeptide (Fig. 3B, lane 4). These findings suggest that in the absence of detergent some N-linked carbohydrate was inaccessible to the enzyme. The  $\approx 50$  kDa molecular weight is lower than expected for nonglycosylated NIS (65.2 kDa), a common finding in the electrophoretic behavior of highly hydrophobic integral membrane proteins (12–14). This anomalous electrophoretic mobility might be due to high binding of detergent, preservation of secondary structure resulting in incomplete protein unfolding, or a combination of both.

Membrane fractions prepared from NIS-expressing COS cells and oocytes were subsequently analyzed. Treatment of COS cells with *N*-glycanase in the absence of detergent (Fig. 3B, lane 6) produced a shift in the relative mobility of the  $\approx 90$ -kDa polypeptide to  $\approx 70$  kDa, and in the  $\approx 55$  kDa polypeptide to  $\approx 50$  kDa. This indicates that even the  $\approx 55$ -kDa polypeptide contains some *N*-linked carbohydrate moieties.

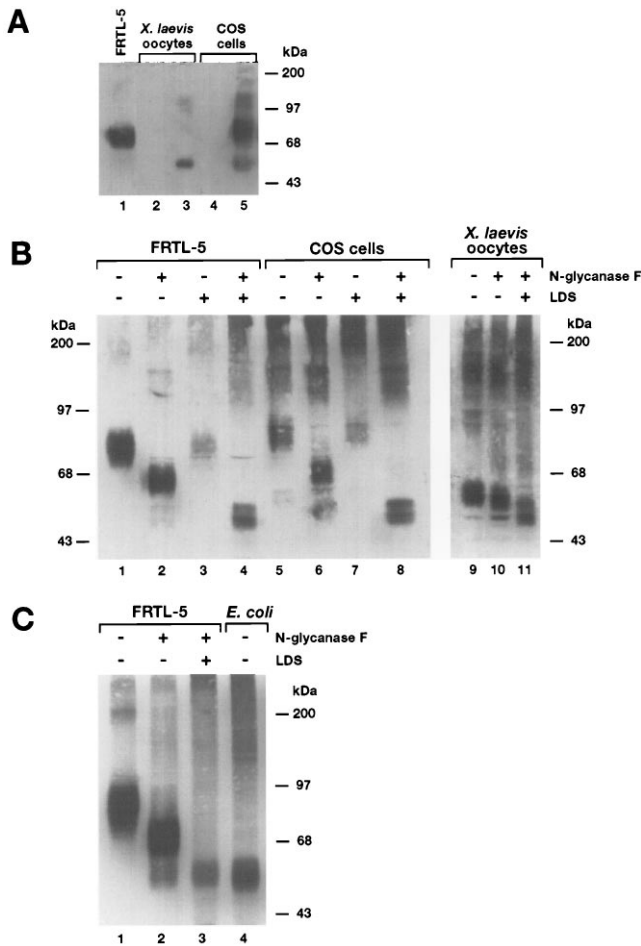


**FIG. 3.** (A) Immunoblot analysis of membranes prepared from either NIS-injected oocytes or transfected COS cells. Membranes from FRTL-5 cells, COS cells, or oocytes were isolated as described. Immunoblot analysis with anti-NIS Ab was conducted as described. Lane 1, FRTL-5 membranes; lane 2, water-injected oocytes; lane 3, NIS cRNA-injected oocytes ( $\approx 50$  ng); lane 4, untransfected COS cells; lane 5, transfected COS cells. All samples contained  $\approx 40$   $\mu\text{g}$  of total membrane protein. (B) Immunoblot analysis of membranes treated with peptidyl *N*-glycanase F. Membranes from FRTL-5 cells, COS cells, and oocytes were prepared as described. Immunoblot analysis with anti-NIS Ab was conducted as described. SDS/PAGE and immunoblot analyses were carried out exactly as described in Fig. 2. Samples ( $\approx 80$   $\mu\text{g}$  of total protein) were incubated either with or without *N*-glycanase in the presence or absence of LDS overnight at 37°C as described. Lanes 1–4, FRTL-5 membranes; lanes 5–8, COS cell membranes; lanes 9–11, oocyte membranes. In lanes 1, 3, 5, 7, and 9, *N*-glycanase was not present; in lanes 3, 4, 7, 8, and 11 (0.1%) LDS was included in the incubation. (C) Lane 1, FRTL-5 membranes without *N*-glycanase or (0.1%) LDS; lane 2, FRTL-5 membranes with *N*-glycanase, without LDS; lane 3, FRTL-5 membranes with *N*-glycanase, and (0.1%) LDS; lane 4, IPTG-treated *E. coli* membranes ( $\approx 30$   $\mu\text{g}$ ). Immunoblot analysis in C was conducted with affinity-purified anti-NIS antibody.

Significantly, in the presence of LDS both the  $\approx 90$ - and  $\approx 55$ -kDa species were converted into  $\approx 50$  kDa species (Fig. 3B, lane 8), suggesting that when presumably all the N-linked carbohydrate moieties are accessible the resulting unglycosylated species is the same, regardless of the extent of processing prior to enzyme treatment. As noted above, this was also the case in FRTL-5 cells. Furthermore, similar results were obtained when NIS-expressing oocytes were analyzed (Fig. 3B, lanes 9–11). It is important to point out that the relative molecular weight of NIS expressed in IPTG-induced *E. coli* is also  $\approx 50$  kDa, indicating that all  $\approx 50$  kDa immunoreactive polypeptides observed in the various cell systems correspond to nonglycosylated NIS (Fig. 3C, lanes 3 and 4). No immunoreactive polypeptides were detected in noninduced *E. coli* (data not shown).

In conclusion, treatment with the enzyme caused the  $\approx 87$ -kDa immunoreactive species to disappear from the immunoblots, apparently converting all putative NIS into a  $\approx 69$ - or  $\approx 50$ -kDa species, depending on the absence or presence of detergent (Fig. 3). Although the  $\approx 55$ -kDa polypeptide is closer to the predicted molecular weight of nonprocessed NIS (65.2 kDa), treatment with *N*-glycanase in the presence of LDS yielded a faster migrating polypeptide of  $\approx 50$  kDa, showing that the  $\approx 55$  kDa form is partially glycosylated and that the polypeptide without N-linked carbohydrate migrates faster than expected in SDS gels.

**Biogenesis of NIS.** To ascertain the relative molecular weight of the NIS precursor molecule and follow NIS biosynthesis, FRTL-5 cells were pulse-labeled with [ $^{35}$ S]methionine for 5 min, washed twice with PBS, and subjected to chase periods from 0 to 180 min in the presence of unlabeled methionine. Solubilized [ $^{35}$ S]methionine-labeled proteins were immunoprecipitated with either anti-COOH NIS Ab (Fig. 4, lanes 2–5) or pre-immune sera (Fig. 4, lane 1), denatured, reduced, released from the complex, and subjected to SDS/PAGE. Analysis of autoradiograms containing pulse-labeled NIS with a 10-min chase revealed the NIS precursor to be a broad  $\approx 56$ -kDa polypeptide (Fig. 4, lane 2). By a 60-min chase period a broad  $\approx 87$ -kDa polypeptide band also became apparent, whereas the intensity of the  $\approx 56$ -kDa band decreased (Fig. 4, lane 4). The  $\approx 56$ -kDa precursor disappeared by 180 min, at which time only the  $\approx 87$ -kDa band, presumably fully processed NIS, was visible. Even after a chase period of 48 hr no decrease of the  $\approx 87$ -kDa polypeptide was observed (not shown), indicating that the half-life ( $t_{1/2}$ ) of NIS is more

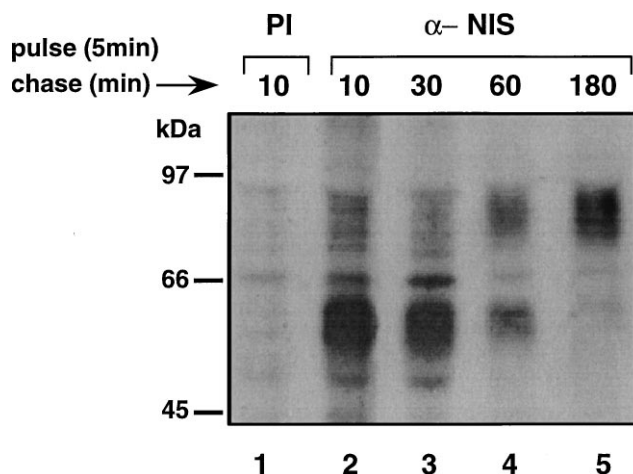


FIG. 4. Biogenesis of NIS. FRTL-5 cells were pulsed for 5 min with [ $^{35}$ S]methionine and chased for the indicated time spans. Cells were harvested and immunoprecipitated with either pre-immune (lane 1) or immune (lanes 2–5) sera as described. Samples were electrophoresed, enhanced, and dried as described. Autoradiogram was exposed for 48 hr at  $-80^{\circ}\text{C}$ .

prolonged than those of most proteins, including transporters such as the norepinephrine transporter ( $t_{1/2}$ , 24 hr; ref. 13).

**In Vivo Regulation of NIS by TSH.** The effect of varying concentrations of serum TSH on the expression of NIS in rat thyroid *in vivo* was explored. Thyroid membrane fractions were prepared from control, PTU-treated, iodine-deficient, and hypophysectomized rats, the latter with or without subsequent injection of bovine TSH. Membrane fractions were subjected to immunoblot analysis with anti-NIS Ab. Because PTU inhibits  $\text{I}^{-}$  organification and therefore the biosynthesis of thyroid hormones, PTU treatment results in an increase of TSH production in the hypophysis (15). Rats subjected to an iodine-deficient diet also develop hypothyroidism and exhibit a compensatory rise in TSH production and release (16). Hypophysectomized rats, which display a very low level of circulating TSH, are a model of secondary (pituitary) hypothyroidism (17). Fig. 5 shows an immunoblot analysis of thyroid membrane fractions from control and experimental rats and from the FRTL-5 cell line as an additional positive control. The expression of NIS corresponds to the  $\approx 90$ -kDa band. Lane 1 displays NIS expression in control (i.e., non-treated) rats. PTU-treated rats and rats subjected to an iodine-deficient diet both exhibited increased NIS expression with respect to control levels (lanes 2 and 3, respectively), whereas hypophysectomized rats exhibited a dramatic reduction in NIS expression (lane 4). Injection of TSH to hypophysectomized rats resulted in restoration of NIS expression back to control levels (Lane 5, HPX + TSH). Thyroidal  $\text{I}^{-}$  transport under these conditions (3, 4) correlated with our observed NIS expression levels. Because of the homogeneity of the preparation, NIS expression in FRTL-5 cells (lane 6) was more pronounced than in thyroid membranes from control animals (lane 1). In conclusion, a direct correlation has been demonstrated between circulating levels of TSH and NIS expression in the thyroid *in vivo*.

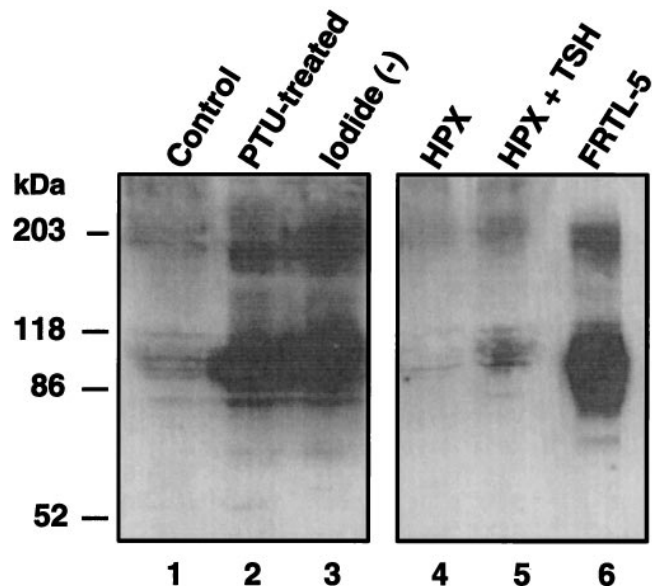


FIG. 5. *In vivo* regulation of NIS. Thyroidectomies were performed on control, experimental, or hypophysectomized female Fisher rats (Charles River Breeding Laboratories). Hypophysectomy was carried out 10–20 days prior to thyroidectomy. Thyroid membrane fractions were subjected to immunoblot analysis with anti-NIS Ab as described in Fig. 1. Thyroid membrane fractions (140  $\mu\text{g}$  of protein) from control rats, lane 1; PTU-treated rats, lane 2; iodide-deficient rats, lane 3; hypophysectomized rats (HPX), lane 4; hypophysectomized rats that received bovine TSH (1 international unit, Calbiochem) administered intraperitoneally 24 hr prior to thyroidectomy (HPX + TSH), lane 5; FRTL-5 membranes (40  $\mu\text{g}$  of protein), lane 6.

The lack of any anti-NIS Abs has until recently been a major stumbling block in the study of this key transporter. The anticarboxyl NIS Ab used here was the first anti-NIS Ab reported (18), whereas an Ab against a Glutathione S-transferase/N-terminal NIS (amino acids 1–231) fusion protein has also been recently obtained (19). The availability of immunological tools and the results presented in this manuscript suggest that long overdue structure/function studies of NIS are now feasible. Such studies are likely to shed light on the iodide transport process at the molecular level.

We thank O. Varlamov and Dr. J. W. McIlroy for their advice in the immunofluorescence experiments, Dr. Pamela Stanley for helpful discussions, and Dr. George Orr for critical reading of the manuscript. O.L. was supported by National Institutes of Health Hepatology Research Training Grant DK-07218. This project was supported by National Institutes of Health Grant DK-41544, American Cancer Society Grant BE-79422, and Thyroid Research Advisory Council (TRAC) of Knoll Pharmaceutical Co. (to N.C.).

1. Stubbe, P., Schulte, F. J. & Heidemann, P. (1986) *Bibl. Nutr. Dieta* **38**, 206–208.
2. Pasquini, J. M. & Adamo, A. M. (1994) *Dev. Neurosci. (Basel)* **16**, 1–8.
3. DeGroot, L. J., ed. (1995) *Endocrinology*, (Grune & Stratton, Orlando, FL), pp. 507–914.
4. Werner, S. C. & Ingbar, S. (1991) in *The Thyroid: A Fundamental and Clinical Text*, eds. Braverman, L. E. & Utiger, R. D. (Lippincott, Philadelphia), pp. 1–1362.
5. Carrasco, N. (1993) *Biochim. Biophys. Acta* **1154**, 65–82.
6. Dai, G., Levy, O. & Carrasco, N. (1996) *Nature (London)* **379**, 458–460.
7. Dai, G., Levy, O., Amzel, L. M. & Carrasco, N. (1996) in *Handbook of Biological Physics. Transport Processes in Eukaryotic and Prokaryotic Organisms*, eds. Konings, W. N., Kaback, H. R. & Lolkema, J. S. (Elsevier, Amsterdam), Vol. 2, pp. 343–368.
8. Carrasco, N., Herzlinger, D., Danho, W. & Kaback, H. R. (1986) *Methods Enzymol.* **125**, 453–467.
9. Ambesi-Impombato, F. S. & Coon, H. G. (1979) *Int. Rev. Cytol. Suppl.* **10**, 163–172.
10. Weiss, S. J., Philp, N. J. & Grollman, E. F. (1984) *Endocrinology* **114**, 1090–1098.
11. Kaminsky, S. M., Levy, O., Salvador, C., Dai, G. & Carrasco, N. (1994) *Proc. Natl. Acad. Sci. USA* **91**, 3789–3793.
12. Newman, M. J., Foster, D. L., Wilson, T. H. & Kaback, H. R. (1981) *J. Biol. Chem.* **256**, 11804–11808.
13. Melikian, H. E., McDonald, J. K., Gu, H., Rudnick, G., Moore, K. R. & Blakely, R. D. (1994) *J. Biol. Chem.* **269**, 12290–12297.
14. Olivares, L., Aragon, C., Gimenez, C. & Zafra, F. (1997) *J. Biol. Chem.* **272**, 1211–1217.
15. Magnusson, R. P., Yu, B. & Brennan, V. (1992) *Acta Endocrinol.* **126**, 460–466.
16. Rognoni, J. B., Penel, C. & Ducret, F. (1984) *Acta Endocrinol.* **105**, 40–48.
17. Chow, S. Y., Kemp, J. W. & Woodbury, D. M. (1982) *J. Endocrinol.* **92**, 371–379.
18. Levy, O., Dai, G., Riedel, C., Amzel, L. M. & Carrasco, N. (1996) in *Thyroid and Trace Elements 6th Thyroid Symposium Proceedings*, eds. Braverman, L. E., Kohrle, J., Eber, O. & Langsteger, W. (Blackwell Wissenschaft, Berlin) (CD-ROM), pp. 104–112.
19. Endo, T., Kogai, T., Nakazato, M., Saito, T., Kaneshige, M. & Onaya, T. (1996) *Biochem. Biophys. Res. Commun.* **224**, 92–95.